

## Nuclear Hyperfine Studies of a Dilute Europous Compound: Europium Hexammine\*

Frederick T. Parker and Morton Kaplan

Carnegie-Mellon University, Pittsburgh, Pennsylvania 15213

(Received 30 March 1973)

The Mössbauer effect of the 21.6-keV  $\gamma$ -ray transition in  $^{151}\text{Eu}$  has been used to investigate the compound  $\text{Eu}(\text{NH}_3)_6$ . Previous magnetic-susceptibility measurements had indicated that the Eu ion might not be in a  $4f^7$  divalent configuration, but in a  $4f^9$  or  $4f^7 5d^2$  condensed state at low temperatures. The present studies strongly support the configuration  $4f^7$ , ionic state  $^8S_{7/2}$ . In contrast to earlier inferences,  $\text{Eu}(\text{NH}_3)_6$  is not magnetically ordered at temperatures as low as 1.2 K. Several unusual features are found to be associated with europium hexammine. The compound has an extremely low Debye temperature of 43 K. It is the only known Eu compound which exhibits magnetic relaxation effects over a wide range of temperatures. The Mössbauer-resonance linewidth (corrected for sample thickness) is approximately constant at 8 mm/sec from 4.2 to 67 K. The broad linewidth indicates spin-spin relaxation and the temperature independence implies an  $\text{Eu}^{2+}$  dipole-dipole relaxation mechanism. Below 4.2 K, the linewidth increases rapidly, probably signifying changes in population of the ionic crystal-field levels. Between 67 and 77 K, the linewidth and recoilless fraction decrease significantly, suggesting a phase change which may be associated with hindered rotation at the  $\text{NH}_3$  sites. The isomer shift,  $-13.6$  mm/sec at 20 K, appears to change slightly with temperature, corresponding to an increasing  $s$ -electron density at the Eu nucleus below about 10 K. From experiments in applied magnetic fields, the limiting hyperfine field is found to be approximately  $-322$  kOe, a value typical for  $4f^7$  core polarization. The spectra obtained in moderate applied fields can be fitted very well using relaxation theory. The exchange field at the Eu ion is less than 0.5 kOe. This implies that the magnetic ordering temperature is less than 0.1 K, one of the lowest for  $\text{Eu}^{2+}$  compounds and unusual because of the material's metallic conductivity. A spin-spin relaxation rate of about  $50 \times 10^6 \text{ sec}^{-1}$  is observed. This is in good agreement with a calculated value  $88 \times 10^6 \text{ sec}^{-1}$ , based upon dipolar interactions and no exchange.

### I. INTRODUCTION

Many divalent and monovalent metals dissolve readily in liquid ammonia yielding characteristic deep-blue solutions. Compounds can be crystallized from the divalent metal solutions with body-centered-cubic (bcc) structures and general formula  $M(\text{NH}_3)_6$ . These hexammines have unusually large lattice constants and are relatively unstable towards chemical decomposition. They are metallic gold in appearance and exhibit high electrical conductivity.

Recent magnetic-susceptibility measurements<sup>1</sup> of  $\text{Eu}(\text{NH}_3)_6$  indicated an unusual temperature dependence of  $1/\chi$ , with a low-temperature (below 47 K) slope corresponding to an ionic moment of about  $10\mu_B$ . This is far larger than the normal moment of about  $7.9\mu_B$ . A mechanism was postulated which could imply enormous consequences for the Eu hyperfine fields; either the configuration  $4f^9$  or  $4f^7 5d^2$  is "frozen out" at low temperatures. The  $4f^9$  configuration, under Hund's rule, is the same as for  $\text{Dy}^{3+}$ . The nuclear magnetic hyperfine field could then be as large as 5 MOe, some ten times larger than in any other Eu compound. The other possibility  $4f^7 5d^2$ , with quenched  $d$ -orbital momentum, could give hyperfine fields some three times larger than expected for typical divalent europium. For  $\text{SmB}_6$ , 70% of the Sm ions are postulated<sup>2</sup> to be in a  $4f^5 (5d_e - 6s)$  state, and

only 30% in the normal  $4f^6$  divalent state. The former divalent state is presumed possible because of the "large" Sm-Sm separation, which is some 10% greater than the metallic diameter of Sm. The  $f^5$  core and the  $5d$ - $6s$  spin couple to produce a nonmagnetic ground state, in contrast to the presumed enhanced moment reported for  $\text{Eu}(\text{NH}_3)_6$ . In dilute metallic systems, screening of the excess charge at the trivalent-rare-earth site leads to  $5d$  virtual bound states. In susceptibility measurements of rare earths in Au and Ag, the  $5d$  state is apparently nonmagnetic, affecting only a cubic crystal-field parameter.<sup>3</sup> For  $\text{Er}^{3+}$  in Zr, Mössbauer measurements indicate a large enhancement of the hyperfine field,<sup>4</sup> although the exact mechanism is not clear.

In order to clarify the Eu ionic configuration and investigate the associated magnetic hyperfine interaction, an extensive study of  $\text{Eu}(\text{NH}_3)_6$  was conducted using the Mössbauer effect of the 21.6-keV  $\gamma$ -ray transition in  $^{151}\text{Eu}$  as a microscopic probe. Experiments were performed in the temperature range 1.2–77 K with and without applied magnetic fields. The nuclear  $\gamma$ -resonance spectra were very sensitive to Eu impurities and decomposition products, and samples were prepared in several different ways to distinguish extraneous effects. With the pure compound, exchange interactions are found to be much smaller than indi-

cated by the macroscopic susceptibility and magnetization measurements, and magnetic ordering was not observed. With a large lattice constant<sup>1</sup>  $a_0 = 9.55 \text{ \AA}$  and nearest-neighbor Eu-Eu distance of about  $8.3 \text{ \AA}$ , paramagnetic relaxation effects were anticipated and have been examined in considerable detail. It is interesting to note that  $\text{Eu}(\text{NH}_3)_6$  can be considered to be almost as "magnetically dilute" as 1-at.%  $\text{Eu}^{2+}$  in  $\text{CaF}_2$ , for example, where the average Eu density is about ten times less but the nearest-neighbor shell at  $3.86 \text{ \AA}$  has about an 11% probability of containing an  $\text{Eu}^{2+}$  ion.

In following sections, the experimental procedures are described, followed by a presentation of the results. First to be considered are the <sup>151</sup>Eu recoilless fraction, Mössbauer linewidth, and isomer-shift measurements as functions of temperature in the absence of external magnetic fields. Next, the saturation magnetic properties of  $\text{Eu}(\text{NH}_3)_6$  are derived from data taken in large applied fields. Then the magnetic relaxation effects are investigated using intermediate strength applied fields. A theoretical description of the relaxation process is introduced since the relaxation-rate and exchange-field parameters are model dependent. Finally, there is a brief discussion of the apparent lack of magnetic exchange.

## II. EXPERIMENTAL

Europium hexammine, prepared by the direct reaction of the metal with liquid ammonia, is a relatively unstable compound. The hexammines decompose reversibly to the metal at sufficiently high temperatures, and irreversibly to the amide  $M(\text{NH}_2)_2$ .<sup>5</sup> The latter reaction should be sufficiently slow (for a catalyst-free system at low temperatures) to have a negligible effect on observed Mössbauer-resonance spectra. In addition, the  $\text{Eu}^{2+}$  ion reacts readily with external contaminants such as water vapor. A further experimental complication lies in the possible nonstoichiometry of the ammine compound. For the isomorphous alkaline earth hexammines, the number of  $\text{NH}_3$  molecules per metal ion is reported to deviate significantly from six.<sup>6</sup>

Because of the above potential difficulties in preparing and keeping  $\text{Eu}(\text{NH}_3)_6$ , special precautions were taken to avoid undesired contaminants and to maintain the material at low temperatures. All operations in the synthesis and subsequent mounting of the compound were carried out under an argon atmosphere in a glove box. Samples for study were prepared in several different ways to give an experimental indication of the possible interference from decomposition products or impurities. The common details will be described first. Eu metal, 99.9% or 99.99% purity (obtained

from United Mineral and Chemical Corp.), was scraped clean of its oxide coating, then cleaned in hexane. The ammonia (99.99% purity, Matheson, Inc.) was singly distilled from Na metal, using a liquid-nitrogen cold trap as a condenser. The Eu metal was placed in a cleaned Plexiglas absorber holder, and the distilled ammonia flowed through Tygon tubing and condensed onto it in excess, using a Cu cold finger immersed in liquid nitrogen. After sealing the holder, the ammonia was allowed to melt and dissolve the Eu metal. A deep-blue solution characteristic of the metal-ammonia systems resulted. The holder was then cooled again on the cold finger and the gold color characteristic of the hexammine appeared. From phase diagrams of the Ca-NH<sub>3</sub> system,<sup>7</sup> this transition corresponds to the precipitation of  $\text{Eu}(\text{NH}_3)_6$ , leaving solid  $\text{NH}_3$  behind. The absorber holder was then placed in a brass mount precooled to liquid-nitrogen temperature. Attachment of the sample to the Mössbauer drive apparatus and insertion into a precooled Dewar were done with the absorber below 100 K, ensuring that any decomposition would be slow.

The differences in preparation of the various samples were as follows:

(i) Sample A was prepared from 99.9% Eu metal; sample holder closed with a snap-fit Plexiglas plug, but no vacuum seal was made.

(ii) Sample B was prepared as with sample A, except that after reaction the sample was allowed to warm up to room temperature to drive off the excess  $\text{NH}_3$ . A gold solid resulted, contrary to previous assumptions<sup>1</sup> that  $\text{Eu}(\text{NH}_3)_6$  is a liquid at room temperature.

(iii) In sample E, a vacuum line was introduced into the glove box so that, once the Eu metal (99.9%) was in the absorber holder, the sample was isolated from the glove box environment. A Plexiglas tube was used for entry into the absorber holder, and after the  $\text{Eu}(\text{NH}_3)_6$  was obtained, the tube was sealed off thermally.

(iv) Samples I and J were prepared from 99.99% Eu metal. Other than using Eu from a new batch with higher rated purity, all other procedures were the same as for sample E, i. e., synthesis was effected under vacuum-line conditions and the sample holder was sealed off leak tight. As will be seen below, these samples exhibited no impurity (presumably oxide) Mössbauer peaks, either divalent or trivalent, indicating that the oxides came from the metal ingot and not from the method of preparation. The oxides are insoluble in liquid ammonia.<sup>8</sup> Sample I was relatively thick ( $\sim 60 \text{ mg Eu/cm}^2$ ).

As a check on chemical identity, x-ray diffraction data were obtained at 77 K for one sample prepared as in (iv) above. With the sample sealed in its Plexiglas holder and using  $\text{MoK}\alpha$  radiation, the

observed reflections were in good agreement with the bcc structure and lattice constant expected<sup>1</sup> for  $\text{Eu}(\text{NH}_3)_6$ .

The reactive nature of the hexammines necessitates special precautions to avoid buildup of impurities with time. A solution of  $\text{NaNH}_3$  did not etch a Plexiglas surface, so presumably the absorber holder was sufficiently inert to the samples to preclude reaction with them. Over a period of about a month at 77 K, the unsealed sample A exhibited decomposition to the trivalent oxide as shown by the growth in the trivalent Mössbauer impurity peak. Another unsealed sample substantially decomposed in about 2 days at 110 K. This is contrary to previous reports<sup>9</sup> that hexammines open to the atmosphere at 77 K showed no visual change. Part of the difference lies in the sensitivity of the Mössbauer technique to impurities at 77 K. A sealed sample was maintained at dry-ice temperature for several weeks with only slight decomposition to the amide, as evidenced by the color at 77 K.

The Mössbauer-resonance experiments were performed in standard transmission geometry using a Mössbauer spectrometer equipped for low-temperature high-field studies. The room-temperature velocity drive system shared a common vacuum space with the bore of a superconducting magnet, and the whole cryostat assembly was mounted in a Dewar fitted with Mylar windows and coupled to a high-speed pumping line. Temperatures below 4.2 K were obtained by pumping on the liquid-helium bath, with the temperature measurements having an accuracy better than 0.02 K using vapor-pressure thermometry. Using liquid nitrogen, the temperature range 63.5–77 K was covered with an accuracy of about 0.1 K. From 4.2 to 63 K, a small resistive heater was used, and temperatures were measured with a carbon resistor and a Cu-constantan thermocouple. Stability was  $\pm 1$  K at the higher temperatures, and somewhat better below.

The Mössbauer-radiation source consisted of 250-mCi  $^{151}\text{Sm}$  as  $\text{Sm}_2\text{O}_3$ , and the resonant 21.6-keV  $\gamma$  rays were detected with a Kr- $\text{CO}_2$  proportional counter located outside the Dewar. The Mössbauer-velocity spectra were accumulated successively in 512-channel groups of a 4096 channel analyzer which was synchronized with the velocity drive sweep and coupled to a minicomputer. The Mössbauer data were analyzed off line using least-squares-fitting programs. Velocity calibrations were performed with Mössbauer spectra from natural Fe foil and isotopically enriched  $\alpha\text{-Fe}_2\text{O}_3$  powder, employing a  $^{57}\text{Co}$  Mössbauer source attached to the room-temperature end of the velocity drive shaft. This procedure yields an accuracy of better than 1% for the velocity scale. Some of

the data reported here exhibit changes less than this, but from previous experience the velocity parameters are known to remain constant to within 0.3%. Thus, for some of the data, only the statistical errors will be given.

### III. RESULTS AND DISCUSSION

#### A. Recoilless Fraction

With its large lattice constant,  $\text{Eu}(\text{NH}_3)_6$  can be considered to be a weakly bound solid. The melting point for isomorphous  $\text{Ca}(\text{NH}_3)_6$  has been reported as  $-5^\circ\text{C}$ <sup>7</sup> or slightly above room temperature.<sup>10</sup> One thus expects a rapid increase in the strength of the Mössbauer resonance with decreasing temperature. This trend is clearly demonstrated in Fig. 1 which shows the Mössbauer spectra for samples I and E at three temperatures, 77, 4.2, and 1.2 K. In Fig. 1, the resonance absorption in sample I is due solely to  $\text{Eu}(\text{NH}_3)_6$ , with no indication of either divalent or trivalent impurities even at 77 K, where the  $\text{Eu}(\text{NH}_3)_6$  peak is very small. For comparison, the spectra of sample E in Fig. 1 exhibit significant resonances from divalent and trivalent impurities, as can be seen from the absorption peaks at 77 K. The possible origin and effect of these impurities will be discussed more fully later. All resonance peaks in these spectra could be excellently fit with single Lorentzian line shapes. No evidence was found in any of the samples for magnetic ordering down to 1.2 K.

The fraction of  $\gamma$  rays emitted or absorbed without recoil is given by<sup>11</sup>

$$f = \exp\left\{-\frac{3}{2}(E_R/k\Theta)[1 + 4(T/\Theta)^2 Q'(z)]\right\}, \quad (1)$$

where  $E_R$  is the free nucleus recoil energy,  $\Theta$  is the effective Debye temperature of the lattice, and  $Q'(z) = Q'(\Theta/T)$  is a definite integral whose values have been tabulated in Ref. 11. This expression gives the expected temperature dependence of the area of the Mössbauer resonance, which is proportional to the product of the depth and width of the Lorentzian line, if saturation effects can be neglected. If the thin-absorber width of the line is constant, then  $f$  describes the dependence of the depth. Figures 2 and 3 show the measured depth and width for sample I as functions of temperature. In the present case, the thin-absorber width is constant over much of the temperature range investigated.

Both width and depth require correction for saturation. Heberle and Franco<sup>12,13</sup> have recently developed methods to treat the case of arbitrary source and absorber linewidths. The relative transmission is given by

$$I_{\text{tra}}(\gamma, s; x) = \sum_{m=0}^{\infty} \frac{(-s)^m}{m!} Q_m(\gamma, x), \quad (2)$$

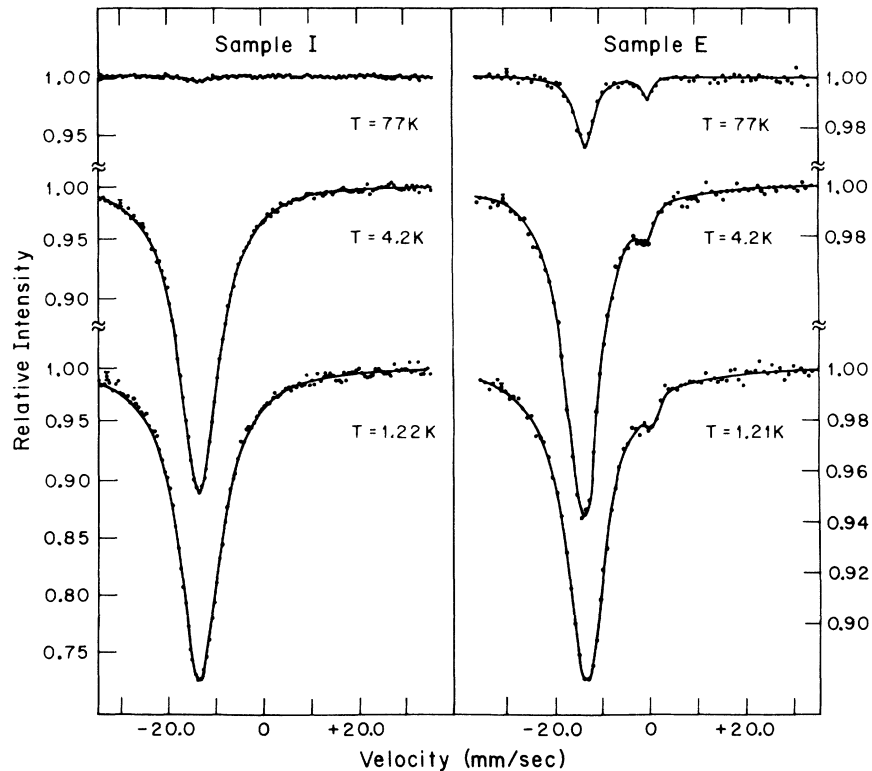


FIG. 1. Mössbauer spectra for two samples of  $\text{Eu}(\text{NH}_3)_6$  at several temperatures. Sample I is effectively free of divalent and trivalent Eu impurities, and exhibits a very small resonance absorption at 77 K as a consequence of the very low Debye temperature. Sample E contains traces of divalent and trivalent impurities, which account for most of the observed resonance absorption at 77 K. The difference in ordinate scales for the two samples is due to sample I being much thicker than sample E.

where  $\gamma = \Gamma_A / \Gamma_s$  is the ratio of absorber to source linewidth and  $s = t / \kappa_A$ , with  $t = n_A f_A \sigma_{\text{res}}$ ,  $n_A$  is the number density of resonant nuclei in the absorber,  $f_A$  is the recoilless fraction, and  $\sigma_{\text{res}}$  is the nuclear cross section for the  $\gamma$  ray at resonance.  $\kappa_A$  is given by  $\Gamma_A = \kappa_A \Gamma$ , with  $\Gamma$  the natural linewidth. The parameter  $x$  is proportional to the energy deviation from resonance, and will be taken as zero. The  $Q_m$  are functions tabulated to sixth order, and all are used here. The quantity measured is the fractional absorption at resonance, given by

$$\epsilon(\gamma, s; 0) = 1 - I_{\text{trans}}(\gamma, s; 0). \quad (3)$$

The relationship for the full width at half-maximum (FWHM) is given by

$$W = W_0 + \frac{1}{4} \Gamma_A s + \Gamma_A^2 s^2 / 32 W_0 - \frac{1}{384} \Gamma_A s^3, \quad (4)$$

where

$$W_0 = (\kappa_s + \kappa_A) \Gamma = \Gamma_s + \Gamma_A \quad (5)$$

is the FWHM for a thin absorber.

Mössbauer measurements with the oxide source against an oxide absorber indicate  $\Gamma_s \approx 1.4$  mm/sec. From sample E (a thin absorber) at 4.2 K, with a FWHM ( $W_0$ ) of 8.60 mm/sec,  $\gamma$  is found to be about 5.0. This ratio is slightly high due to saturation. The expressions for  $W$  and  $\epsilon$  were manipulated to obtain the best fits for the data in

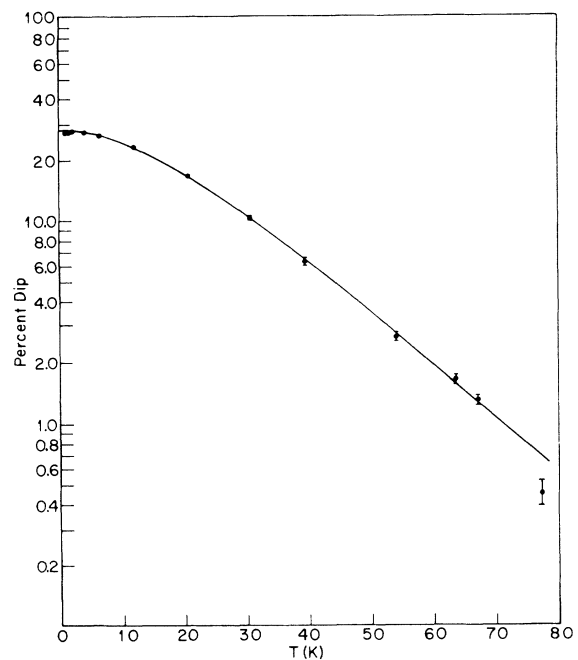


FIG. 2. Temperature dependence of fractional resonance depth for sample I. The solid curve represents the Debye model prediction with a Debye temperature  $\Theta = 43$  K and a thickness saturation parameter  $s = 1.12$  at 4.2 K.

Figs. 2 and 3, using as independent variables  $s$  (evaluated at 4.2 K),  $\Theta$ , and  $\Gamma_A$ . For computer purposes, an approximation for  $f$  was used<sup>14</sup>:

$$f = \exp\left\{-\frac{3}{2}(E_R/k\Theta)[1 + 4(T/\Theta)^2(Q(z) + E(z))]\right\}, \quad (6)$$

with  $Q(z)$  and  $E(z)$  given in Ref. 14. The final results are shown as the solid curves in Figs. 2 and 3, with the parameters

$$\Theta = 43.0 \text{ K}, \quad s = 1.12 \text{ (at 4.2 K)}, \quad W_0 = 7.9 \text{ mm/sec}, \\ \Gamma_A = 6.5 \text{ mm/sec}, \quad \gamma = 4.65.$$

As can be seen, the agreement with the experimental data is very satisfactory.

The accuracy for  $\Theta$  is estimated to be about  $\pm 1$  K; an absolute upper limit ( $s^2 \equiv 0$ ) is 46 K. Using the observed dip for sample E at 4.2 K, the FWHM is predicted to be about 8.5 mm/sec, in excellent agreement. Thus, over most of the temperature range, the thin-absorber FWHM [Eq. (5)] is indeed constant. Sources of error for the  $\Theta$  measurement include the temperature uncertainties, some very slight drift in the  $\gamma$ -ray window, and slightly different (although still weak) backgrounds under the 21.6 keV  $\gamma$ -ray peak when using liquid helium and liquid nitrogen in the Dewar. In addition, the source temperature varies approximately with the absorber's, which changes the recoilless fraction in the source. Since  $\Theta \approx 240$  K for  $\text{Sm}_2\text{O}_3$ ,<sup>15</sup> this yields an additional approximate 7% change in the range 4–77 K, which can be neglected.

The derived Debye temperature of  $\text{Eu}(\text{NH}_3)_6$  is remarkably low. For  $\text{Li}(\text{NH}_3)_4$ , heat-capacity measurements<sup>9</sup> yield  $\Theta \approx 55$  K at 0 K, and there is some indication that  $\Theta$  decreases with increasing temperature. Different techniques of measuring

Debye temperatures usually given different results due to the varying dependence on lattice frequencies, but considering that Eu is more massive than Li, a lower  $\Theta$  is expected in  $\text{Eu}(\text{NH}_3)_6$  as is observed.

The anomalous peak (see Fig. 1) from a divalent Eu impurity observed in the samples prepared before sample I showed little change in depth as the temperature varied from 77 K to about 100 K. The FWHM at 77 K was somewhat less than at 63.5 K, much less than at 4.2 K, and nearly down to typical <sup>151</sup>Eu widths. Since the divalent impurity apparently originates in the Eu metal, a good possibility is that finely divided  $\text{EuO}$  ( $\Theta \approx 250$  K)<sup>16</sup> particulates are causing the anomaly. This point will be discussed further in Sec. III C on isomer shifts. From the relative areas at 77 and 4.2 K, at 4.2 K approximately 10% of the Mössbauer spectrum for sample E arises from the divalent impurity, although no anomalous prominences are visible at 4.2 K. The divalent impurity comprises about 6 at. % of the europium in the sample; the trivalent impurity about 2%.

The recoilless fraction of  $\text{Eu}(\text{NH}_3)_6$  follows the expected curve (see Fig. 2) for a Debye model solid quite well except at the highest temperature measured, 77 K. At this temperature, there is a steep drop in percent of effect, and also in FWHM, yielding a resonance area much less than predicted. There is no indication in the susceptibility measurements<sup>1</sup> of a transition at this temperature. The susceptibility data do indicate a transitional region at 47 K which has no counterpart here. As will be covered in Sec. IIIB, the collapse of the linewidth at 77 K is apparently caused by a change in the  $\text{Eu}^{2+}$ - $\text{Eu}^{2+}$  spin-spin relaxation mechanism.

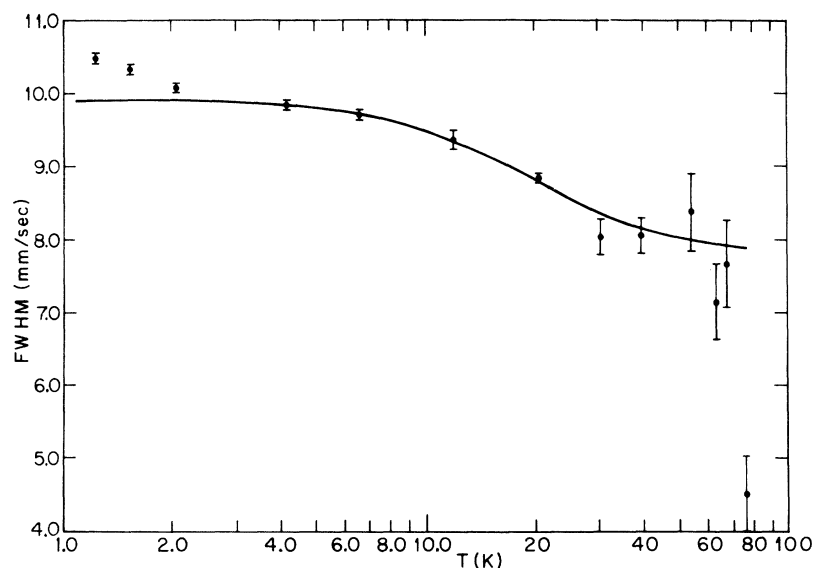


FIG. 3. Temperature dependence of the resonance linewidth for sample I, fit as a single broadened Lorentzian. The same parameters used in Fig. 2 are employed here. The saturation correction works well, indicating that the thin absorber FWHM is constant from about 4.2 to 67 K, broadens below 4.2 K, and apparently narrows above 67 K. (Statistical errors only.)

Since the  $\text{Eu}(\text{NH}_3)_6$  resonance has become so small, impurity effects such as mentioned above could be causing the drop in linewidth. However, the isomer shift remained constant.

### B. Linewidth and Relaxation

As the experimental data indicate a constant thin-absorber linewidth for most of the temperature range investigated, the relaxation mechanism is most likely to be of the  $\text{Eu}^{2+}$  spin-spin type. The relaxation process should not depend on temperature if  $kT \gg E_s$ , where  $E_s$  is the overall crystal field splitting. It is easy to show<sup>17</sup> that the electronic-spin correlation time  $\tau$  is proportional to the linewidth in excess of that expected for very fast relaxation. Another relaxation mechanism, described by the Korringa relation,<sup>18</sup> predicts that the correlation time is inversely proportional to  $kT$ .<sup>19</sup> The perturbation for this type of relaxation is of Ruderman-Kittel-Kasuya-Yosida (RKKY) nature,

$$\mathcal{H}_p = -J_{sf} \vec{S} \cdot \vec{s}, \quad (7)$$

where  $\vec{S}$  is the  $\text{Eu}^{2+}$  spin operator,  $\vec{s}$  is the conduction electron operator, and  $J_{sf}$  is an exchange constant. Since the FWHM (adjusted for saturation) shows no temperature dependence from 4.2 to 67 K, the ionic spin-spin mechanism dominates.

At 77 K, the sharp drop in FWHM could indicate that some higher-order spin-lattice relaxation processes are involved. The temperature dependence of the rate would probably be  $T^5$  (Raman process),<sup>20</sup> which gives approximately the correct narrowing from 67 to 77 K. The anomalous drop in recoilless fraction must then arise from some other mechanism, perhaps the anharmonicity of lattice vibrations expected for  $T$  much larger than  $\Theta$ . Another possibility is a change in site symmetry, which will be covered below.

At temperatures below 4 K, the FWHM begins to broaden. In Fig. 4 the data for sample E are presented. All samples showed similar broadening. To account for this low-temperature variation, the crystal-field splittings must be discussed.

The  $\text{Eu}^{2+}$  ion in cubic symmetry experiences an effective crystal field given by<sup>21</sup>

$$\mathcal{H}_c = B_4(O_4^0 + 5O_4^4) + B_6(O_6^0 - 21O_6^4), \quad (8)$$

where the  $B_n$  are constants and the  $O_n^m$  are operator equivalents for the  $^8S_{7/2}$  ground state. For  $\text{Eu}^{2+}$ , the  $B_n$  are not obtainable from first principles. For example, in the octahedrally coordinated MO series<sup>22</sup> the fourth-order parameter changes sign where the host cation has the same ionic size as  $\text{Eu}^{2+}$ . For our calculations, the available data for  $\text{CaF}_2:\text{Eu}^{2+}$  will be used.<sup>23</sup> Setting  $B_6 \approx 0$ , there are crystal-field levels  $\Gamma_7$ ,  $\Gamma_8$ , and  $\Gamma_6$  in increasing energy, with the over-all splitting  $E_s \approx 0.25$  K.

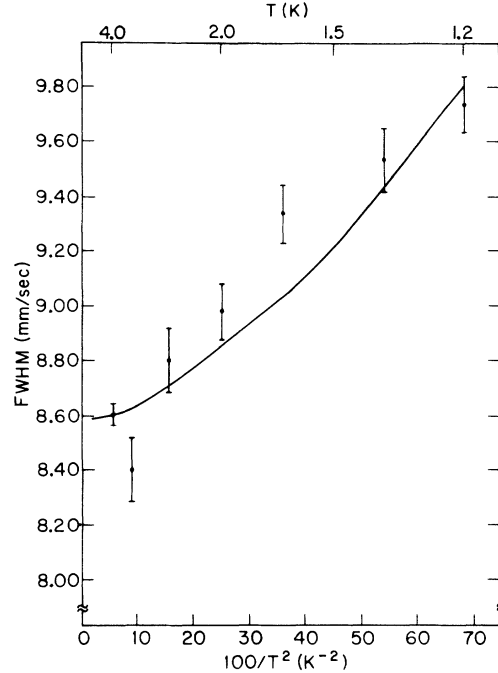


FIG. 4. Temperature dependence of the resonance linewidth for sample E below 4.2 K. The solid line represents the dependence expected for a cubic  $\text{Eu}^{2+}$  site symmetry,  $\Gamma_7$  ground state, with some simplifying assumptions including  $g_L = 0$ . This gives an over-all cubic crystalline-field splitting of about 2.5 K, which is much larger than expected. (Statistical errors only.)

The  $\Gamma_8$  level is a quartet, and the other two are doublets.

The increasing linewidth at low temperatures does not agree very well with calculations based upon cubic site symmetry, as can be seen from the following. For a simple model, the assumptions are (i) relaxation can proceed only between levels; (ii) the relaxation matrix elements are the same; (iii) the effective hyperfine fields (proportional to  $\langle S_x \rangle$ ) for the three levels are equal; and (iv) that the nuclear and electronic spins are effectively decoupled by a weak exchange and/or dipolar field. The rate can be taken as proportional to the suitably weighted Boltzmann occupation factors, and the FWHM obtained from the inverse plus the fast-relaxation FWHM. With this model, the relaxation rate slows down as available paths are decreased; a value  $E_s \approx 2.5$  K is obtained. The solid curve in Fig. 4 exhibits the predicted temperature dependence with  $\Gamma_7$  as the ground state. This seems to be far too large. Using a  $\Gamma_6$  ground state, the curve is more nearly linear, but with an even larger  $E_s$  of about 3.7 K. Furthermore, one would expect that relaxation of the form  $\Gamma_i \rightleftharpoons \Gamma_j$  should also occur within the cubic levels, since  $g_L \neq 0$  (for

any of the  $\Gamma_i$ ). This would tend to cancel the temperature dependence and make agreement with experiment worse.

The rapid change in linewidth below 4.2 K may be explained by noncubic site symmetry, with the lowest state having  $g_{\perp}=0$ . Assuming only a  $D$  term (axial symmetry) in the crystal-field Hamiltonian, theoretical Mössbauer spectra were generated using a method to be discussed later. Although structure in the calculated spectra was becoming evident, an estimate of  $D \approx -0.03$  K was obtained by comparing relative broadening of theoretical and experimental spectra. A similar value was derived<sup>24</sup> from ESR measurements of  $\text{Eu}^{2+}$  in silver chloride. With the apparent deviation from cubic symmetry, one might expect that a quadrupole splitting could also be present, although no evidence of this was found in the data.

Among the prime candidates for sources of  $D$  is the reported deviation in stoichiometry for hexamines. Another is a possible change in  $\text{Eu}^{2+}$  site symmetry from cubic to trigonal if the rotation of the  $\text{NH}_3$  groups slows to the order of the hyperfine interaction frequencies. A sudden onset of quadrupole splitting is visible in iron(II) hexamine chloride<sup>25</sup> as the temperature is lowered below about 109 K. Bates and Stevens<sup>26</sup> indicate that static arrangements yield trigonal symmetry, and that the chlorine should have little effect on the cooperative transition temperature. Another origin is suggested by the cubic-to-hexagonal transition<sup>27</sup> in  $\text{Li}(\text{NH}_3)_4$  below 82 K. Both of the latter mechanisms would provide sharp changes in the  $\text{Eu}^{2+}$  wave functions.

With the large chemical reactivity of  $\text{Eu}(\text{NH}_3)_6$ , some concern must be given to the effect of possible impurities on the FWHM. The divalent impurity exhibited in the earlier samples (A-E) apparently is not responsible for the broadening,

since samples I and J also broaden. If there were a small amount of impure amide present, with magnetic-ordering temperatures of the various microscopic regions scattered below 4.2 K, an effectively broader line would result. However, sample B should then show the sharpest change since its method of preparation should enhance the formation of amide. Instead, it shows approximately the same temperature dependence below 4.2 K. A slightly narrower line, compared to the other samples, was observed and could arise from a somewhat smaller lattice constant due to a slight  $\text{NH}_3$  deficiency and thus faster relaxation.

Similar Mössbauer line broadening below 4.2 K is observed<sup>28</sup> with  $\text{La}:\text{Eu}^{2+}$ . Below the La superconducting transition temperature, the pairing of the conduction electrons is expected to produce an exponential decrease in relaxation rate. The  $\text{La}:\text{Eu}^{2+}$  data also fit reasonably well with the approximate  $1/T^2$  dependence expected for crystal-field-population effects. A  $1/T$  (Korringa) dependence is also possible, unless " $T_0$ " is not the fast relaxation limit.

### C. Isomer Shift

The experimental isomer shift results for sample I are plotted as a function of temperature in Fig. 5. At the higher temperatures, the isomer shift is relatively constant at about  $-13.6$  mm/sec with respect to the  $\text{Sm}_2\text{O}_3$  source. The isomer shift shows a gradual, but accelerating trend towards more positive values as the temperature decreases. At 21 K the isomer shift is  $-13.62 \pm 0.02$  mm/sec (statistical error only). At 4.2 K it is  $-13.54 \pm 0.01$  mm/sec, and at 1.22 K it has increased to  $-13.38 \pm 0.02$  mm/sec. This "isomer-shift shift" (ISS) corresponds to increasing  $s$ -electron density at the Eu nucleus at lower temperatures. There are some experimental data

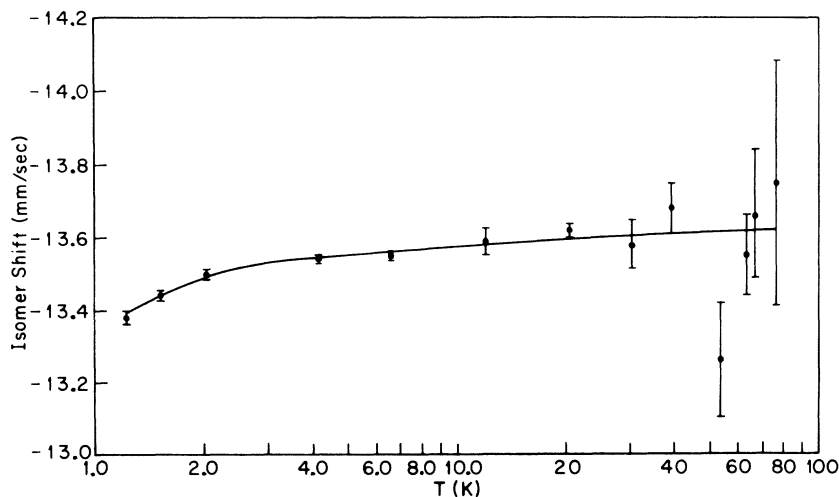


FIG. 5. Temperature dependence of the Mössbauer isomer shift for sample I, referred to an  $\text{Sm}_2\text{O}_3$  source. A trend towards more positive values is visible at lower temperatures. The solid curve is based on an apparent change in conduction electron density, as suggested for  $\text{Li}(\text{NH}_3)_4$ . (Statistical errors only.)

which provide a possible explanation of the ISS. In the hexagonal phase of  $\text{Li}(\text{NH}_3)_4$ ,<sup>27</sup> below 82 K, there are two Li atoms per unit cell and likely contact between the Fermi surface and the Brillouin-zone boundary. At low temperatures,  $\text{Li}(\text{NH}_3)_4$  thus has some characteristics, such as complete compensation, similar to a divalent metal<sup>29</sup> or to  $\text{Eu}(\text{NH}_3)_6$ . Recent Hall-effect measurements<sup>30</sup> show that the number density ( $n_e$ ) of electrons is much less than that ( $n_0$ ) calculated on the basis of one electron per Li atom. At 77 and 62 K,  $n_e/n_0 \approx 4.4 \times 10^{-3}$ . Below 47 K the ratio increases, reaching  $4.9 \times 10^{-2}$  at 1.5 K. The  $\text{Eu}^{2+}$  isomer shift is usually interpreted as arising from two parts; a negative shift of about  $-15$  mm/sec due to the  $4f$  shielding for  $\text{Eu}^{2+}$ , and a positive contribution of 15 mm/sec per  $6s$  conduction electron per ion.<sup>31</sup> The solid curve in Fig. 5 was obtained by scaling the results from  $\text{Li}(\text{NH}_3)_4$ , using  $-13.64$  mm/sec as the no-conduction electron limit. The 1.5-K data point corresponds to  $n_e/n_0 \approx 1.3 \times 10^{-2}$   $6s$  electron. The ratio should be less here than in  $\text{Li}(\text{NH}_3)_4$  since only the  $s$  part of the conduction band is significant. The high-temperature limit  $-13.64$  mm/sec is typical of the nonionic, nonmetallic divalent Eu compounds, and is probably indicative of some covalent bonding of the  $4f$  or  $5p$  shell of  $\text{Eu}^{2+}$  with the nitrogen ligands.

Recently, an ISS was observed in Eu-rich  $\text{EuO}$ .<sup>32</sup> As the exchange field increases below the  $\text{EuO}$  Curie temperature, the model envisions that the electron- $\text{Eu}^{2+}$  magnetic localization energy is lost, and metallic conductivity occurs. Conductivity data indicate a net increase in conduction electrons to  $n_e \approx 2 \times 10^{19} \text{ cm}^{-3}$ . The ISS is about  $+0.15$  mm/sec, from  $-12.25$  mm/sec at 70 K to  $-12.10$  mm/sec at 50 K. Assuming that  $n_e$  represents idealized free  $s$  electrons, this indicates an expected shift of about 0.01 mm/sec, far less than observed.

For the absorbers other than samples I and J, the isomer shifts at 77 K were all about  $-12.6$  mm/sec, and at 63.5 K,  $-13.0$  mm/sec. These values are considerably more positive than found for the pure samples (I and J), and indicate the sensitivity to impurities. The trend to more negative isomer shifts as the temperature is lowered indicates that the  $\text{Eu}(\text{NH}_3)_6$  Mössbauer effect becomes more important than the impurity effect as its recoilless fraction increases. The isomer shift at 77 K is slightly more negative than that in  $\text{EuO}$ ,<sup>32</sup>  $-12.2$  mm/sec. In addition, the Mössbauer resonance has broadened substantially at 63.5 K, but nearly full hyperfine splitting would be expected if the impurity were pure  $\text{EuO}$  with a Curie temperature of 69.2 K.<sup>33</sup>

At 4.2 K and below, the  $\text{Eu}(\text{NH}_3)_6$  resonance is dominant. Low-temperature isomer-shift results for several samples are shown in Fig. 6. All sam-

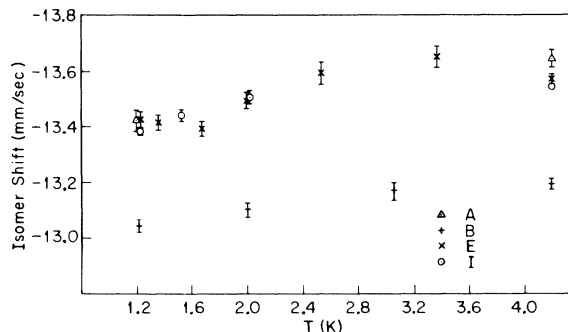


FIG. 6. Temperature dependence of the observed isomer shifts for samples A, B, E, and I below 4.2 K. Since various means of preparation and amounts of impurities are represented, the temperature dependence is most likely not due to an impurity effect. (Statistical errors only.)

ples show a shift towards more positive values as the temperature is lowered, indicating that the impurity contribution is not a significant factor. The isomer shift for sample B appears to be more positive than the others, even when one allows for a possible variation of 1% in absolute velocity calibration between samples. Recall that sample B was warmed to room temperature to drive off all excess ammonia, and hence may contain some decomposition products.

There are several other mechanisms which are unable to account for the observed temperature-dependent shift. The postulated  $4f^7 5d^2$  condensation model requires a net reduction in  $s$ -electron density. The second-order Doppler shift is far too small. Lattice contraction at low temperatures, which could give a positive shift,<sup>34</sup> would cause a width decrease. The orbit-lattice interaction admixes the  $4f^6 6s$  configuration into the  $4f^7$  ground state with increasing temperature,<sup>35</sup> and this increases the isomer shift. A Debye-model calculation indicates a variation at  $T = 43$  K of about 0.02 mm/sec, too small to be observed here.

By fitting the experimental data with a single Lorentzian function, an apparent ISS would be observed if, for example, quadrupole splitting or off-diagonal terms in the hyperfine interaction changed significantly with temperature. A similar effect could occur from a change in the spin relaxation rate. Presumably, the data should exhibit some asymmetry under these conditions. A further discussion of this ISS origin will be given later.

#### D. Induced Hyperfine Fields

It appears that  $\text{Eu}(\text{NH}_3)_6$  does not order magnetically for  $T \geq 1.2$  K. None of the samples (including sample B which was free of excess  $\text{NH}_3$  and samples I and J which were free of Eu impurities)

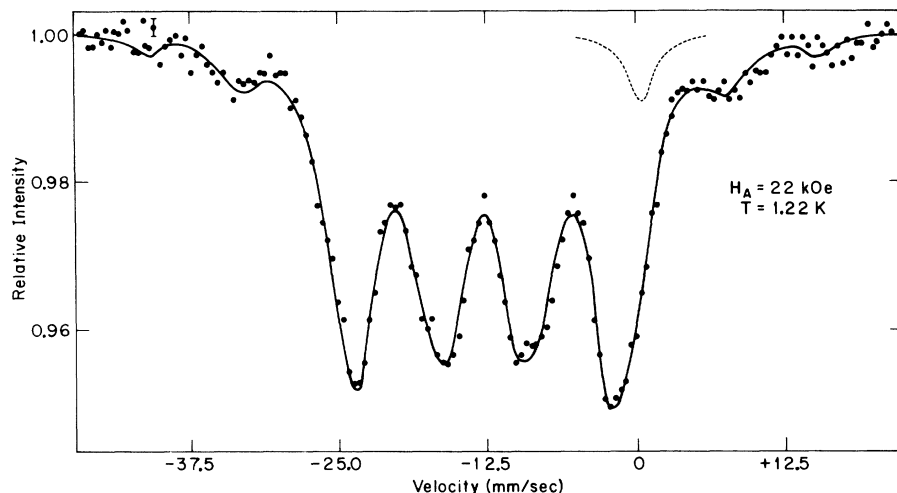


FIG. 7.  $\text{Eu}(\text{NH}_3)_6$  Mössbauer spectrum at  $H_A = 22$  kOe,  $T = 1.2$  K (sample B). With essentially only the ground  $S_z$  level populated, a normal magnetic Hamiltonian was used to fit the data, with the constraint that the  $\Delta M_I = 0$  transitions have zero intensity in the longitudinal field. A small trivalent impurity is indicated by the dashed curve. For this particular spectrum, the source was in a magnetic field, which resulted in some broadening of the lines.

gave any indication of hyperfine splitting in the Mössbauer spectra. However, some  $\text{EuM}_2$  ( $M$  a transition metal) intermetallic compounds show very small hyperfine fields in the ordered state.<sup>36</sup> In order to obtain the hyperfine fields corresponding to a fully magnetized state, Mössbauer experiments were carried out in large external fields at 1.2 K. An example of the observed data is shown in Fig. 7 for sample B at  $H_A \cong 22$  kOe,  $T = 1.22$  K. The solid curve denotes a least-squares fit to a pure magnetic Hamiltonian for  $\text{Eu}^{2+}$  and a single-line trivalent impurity. With the external magnetic field applied along the observation axis, the  $\Delta M_I = 0$  transitions are eliminated and the fit in Fig. 7 assumes this constraint. As can be seen, the agreement is excellent. In a later section, somewhat smaller  $H_A/T$  data require the use of relaxation parameters. For the present data, the occupation of the ground ionic  $\text{Eu}^{2+}$  level is about 90%, and the assumption of "fast" relaxation is adequate for fitting purposes.

For large external fields, the observed effective hyperfine field decreases with increasing applied field. Figure 8 shows this variation for sample E at  $T = 1.2$  K. The fitted line is given by

$$H_{\text{eff}} = H_A + 312 \langle S_z \rangle / 3.5 \text{ kOe}$$

and the net hyperfine magnetic field which would be expected in the fully magnetized  $\langle S_z \rangle = -\frac{7}{2}$  state is  $H_{\text{eff}} = -312 \pm 7$  kOe. The small demagnetizing fields (and a possible weak exchange field) are less than the statistical errors and will be ignored here.

This value of saturation field is typical for  $\text{Eu}^{2+}$  compounds.<sup>37</sup> The  $4f$  core polarization of the filled  $s$  shells yields about  $-340$  kOe,<sup>38</sup> and typically fields slightly more positive are observed. For the postulated  $4f^9$  configuration, with a ground term  ${}^6H_{15/2}$  and a magnetic moment of  $10\mu_B$ , the orbital angular momentum would dominate. The satura-

tion hyperfine field would then be<sup>39</sup> about 5 MOe. The other suggested possibility  $4f^7 5d^2$  would yield fields dependent on the orbital quenching of the  $t_{2g}$   $d$  electrons. If there is total quenching, the core polarization induced by the  $5d$  electrons would dominate. With a  $5d$  core-polarization field<sup>40</sup> of  $-550$  kOe/gS, and assuming that the  $4f$  and  $5d$  core polarization fields are additive, a net hyperfine field of about  $-1.45$  MOe would be expected. Further evidence for a  $4f^7$  configuration lies in the magnetization measurements.<sup>1</sup> Extrapolation of  $\mu$ -vs- $1/H$  curves indicate the saturation moment is about  $7.0\mu_B$ , which is expected for  $\text{Eu}^{2+}$ . If  $\text{Eu}(\text{NH}_3)_6$  were magnetically ordered, the approach to saturation could depend on anisotropy or spin canting. Since it is not ordered, the magnetization measurements indicate a  $4f^7$  configuration.

There are small differences in the hyperfine

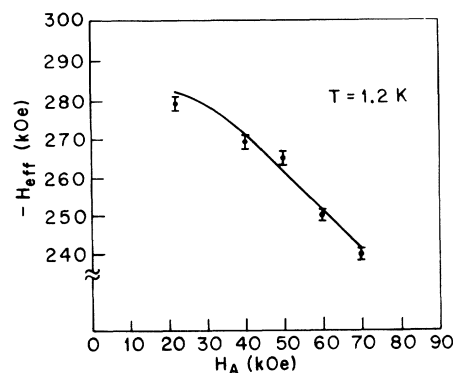


FIG. 8. External field dependence of the magnetic hyperfine field in sample E. The solid curve represents an effective hyperfine field of  $-312$  kOe. For the lowest values of external field, a Boltzmann average was employed. This assumes "fast" relaxation, which is sufficient for the small populations in the excited Zeeman levels.

TABLE I. Comparison of derived saturation hyperfine fields for  $\text{Eu}(\text{NH}_3)_6$ .

Sample	$H_{\text{eff}}$ (kOe)
A	-315
B	-303
E	-316
I	-323
J	-321

Velocity calibration error is  $\pm 3$  kOe

fields observed for the various samples studied. For comparison purposes, most samples were run at an external field of about 20 kOe at 1.2 K. In Table I the results for samples A-J are presented, corrected for net ionic magnetization and external field. The data for sample J were taken at 60 kOe, 1.2 K, and are corrected for external field only. The lowest field for sample B could result from impurities produced by warming the sample to room temperature. Samples A and E were similarly prepared (except for the somewhat cleaner method used for sample E) and exhibit the same field. Samples I and J exhibit a somewhat larger hyperfine field. Since they exhibited no divalent impurity, the lower fields observed in A and E could be caused by the possible admixture of small amounts of EuO impurity. Pure EuO has a somewhat lower saturation field<sup>33</sup> than  $\text{Eu}(\text{NH}_3)_6$ ; in the present case, the field could be reduced and vary somewhat due to a deviation from stoichiometry.

Since there is a possibility of a  $D$  term in the ionic Hamiltonian, an attempt was made for sample-B data to include a quadrupole hyperfine interaction of the form<sup>41</sup>

$$\Delta W_Q = \frac{eQV_{zz}}{4} \frac{3M_I^2 - I(I+1)}{I(2I-1)} \left( \frac{3}{2} \cos^2 \alpha - \frac{1}{2} \right), \quad (9)$$

where  $\frac{1}{4}eQV_{zz}$  is the quadrupole interaction parameter and  $\alpha$  is the local angle between the magnetic and quadrupole axes. Since the sample was not a single crystal, a suitable grid in angles was chosen, and the resultant Mössbauer spectrum was obtained as the weighted average over this grid. The fit was found to be too insensitive to this quadrupole perturbation, with only a slight broadening for large values of  $\frac{1}{4}eQV_{zz}$ .

#### E. Intermediate External Fields-Relaxation Spectra

Mössbauer spectra of  $\text{CaF}_2:\text{Eu}^{2+}$  exhibit<sup>42</sup> broad zero-field resonances as well as relaxation phenomena for small values of  $H_A/T$ . Similarly, the spectra for  $\text{Eu}(\text{NH}_3)_6$  shown in Figs. 9 and 10 exhibit the typical non-Lorentzian shapes expected for time modulation of the hyperfine field resulting from relaxation effects. Figure 9 represents the

data for sample J at 4.2 K in applied fields  $H_A$ , as indicated. The results at lower temperatures in applied fields are given in Fig. 10. For both figures, the line shapes (solid curves) were calculated

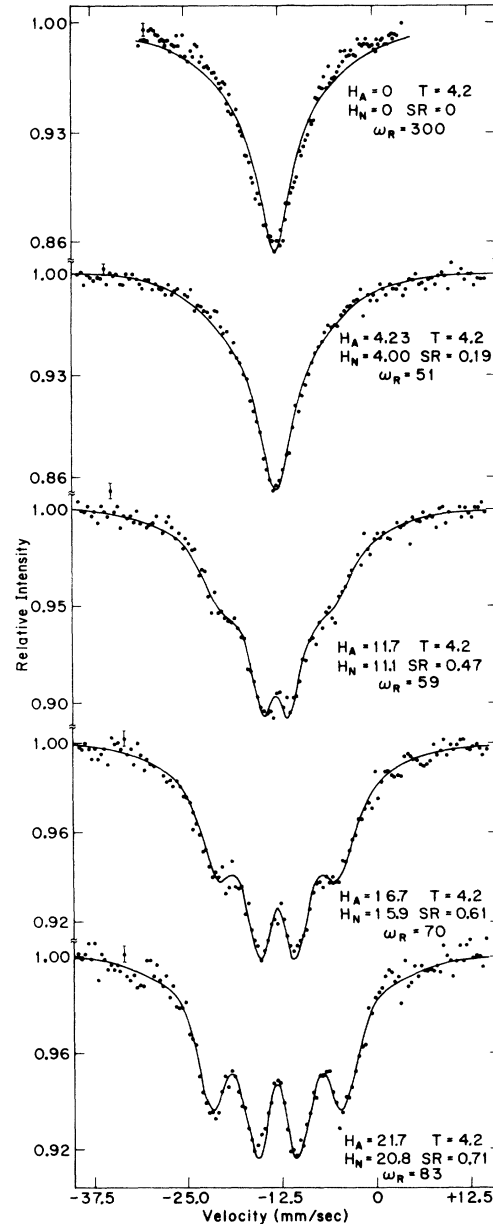


FIG. 9. Mössbauer spectra of  $\text{Eu}(\text{NH}_3)_6$  (sample J) at 4.2 K in applied magnetic fields  $H_A$ . The solid curves are theoretical relaxation spectra with the indicated values of the parameters  $H_N$ , the net ionic field,  $SR = -\langle S_z \rangle / 3.5$ , and  $\omega_R$ , the spin-spin relaxation frequency. For the  $H_A = 0$  data, single-level relaxation is employed. The other spectra were derived using the multilevel formalism. The parameters indicated in the figure are in units of kOe for  $H_A$  and  $H_N$ ,  $^\circ\text{K}$  for  $T$ , and  $10^6 \text{ sec}^{-1}$  for  $\omega_R$ .

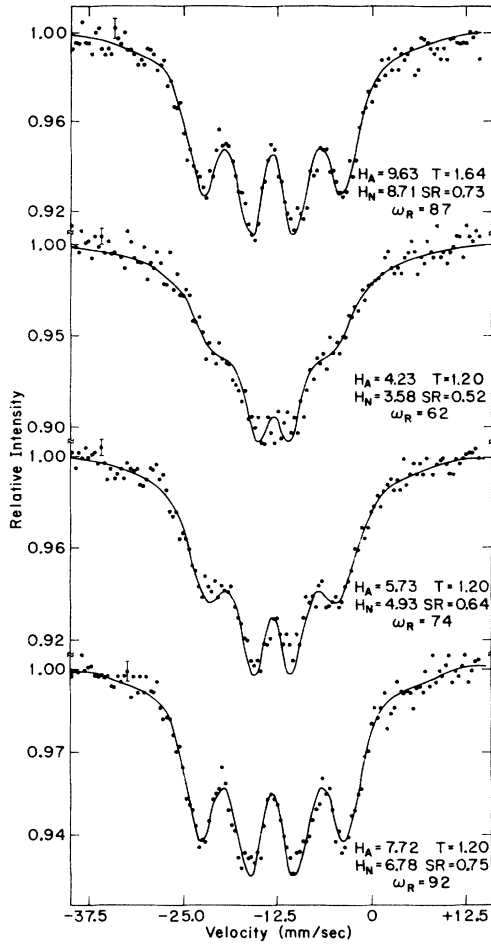


FIG. 10. Mössbauer spectra of  $\text{Eu}(\text{NH}_3)_6$  (sample J) in applied magnetic fields at temperature below 2 K. The solid curves are theoretical relaxation spectra, with the defined parameters and units as for Fig. 9.

by the rate equation method.<sup>43</sup> The agreement with experiment is amazingly good, and yields the parameters shown in the figures. These will be discussed more fully below, after presentation of the necessary theory.

From Van Vleck,<sup>44</sup> in the case of zero crystal field and external field large compared to the dipolar field, the spin Hamiltonian can be written

$$\mathcal{H} = g\mu_B H_N \sum_j S_z^j + \sum_{k>j} A_{jk} \vec{S}^j \cdot \vec{S}^k + \sum_{k>j} B_{jk} S_x^j S_x^k, \quad (10)$$

where  $H_N$  is the net ionic field,

$$A_{jk} = -2J + g^2 \mu_B^2 \gamma_{jk}^{-3} (\frac{3}{2} \alpha_{jk}^2 - \frac{1}{2}), \quad (11)$$

and

$$B_{jk} = -3(A_{jk} + 2J).$$

$J$  is the isotropic exchange parameter,  $\gamma_{jk}$  the

separation of ions  $j$  and  $k$ , and  $\alpha_{jk}$  is the cosine of the angle between the external field and the  $j$ - $k$  axis.

Considering only the second term of Eq. (10), the spin-flip part of the Hamiltonian for ion  $k$  is

$$\mathcal{H}_{CS} = - \sum_j [J + \frac{1}{4} G_{jk} (1 - 3\alpha_{jk}^2)] (S_+^k S_-^j + S_-^k S_+^j), \quad (12)$$

with  $G_{jk} = g^2 \mu_B^2 \gamma_{jk}^{-3}$ . The probability for a transition  $M_k \rightarrow M'_k$  with a neighboring ion  $j$  going from  $M_b \rightarrow M'_b$  is then<sup>45,46</sup>

$$P(M_k \rightarrow M'_k) = \frac{2\pi}{\hbar} \sum_j [J + \frac{1}{4} G_{jk} (1 - 3\alpha_{jk}^2)]^2 \times \sum_{M_b} |\langle M'_k, M'_b | S_+^k S_-^j + S_-^k S_+^j | M_k, M_b \rangle|^2 \times P(M_b) P(E), \quad (13)$$

where  $P(M_b)$  is the Boltzmann probability for occupation of the  $M_b$  state at ion  $j$  and  $P(E)$  is the level density, taken as the inverse linewidth of the ionic levels.

In the absence of exchange, the ionic linewidth arises solely from the third term in the Van Vleck Hamiltonian. For a polycrystal, the mean-square frequency averaged over angle is

$$\langle \Delta\nu^2 \rangle_{av} = \frac{3}{5} \hbar^{-2} S(S+1) \sum_j G_{jk}^2. \quad (14)$$

Inserting the dependence on ionic occupation<sup>47</sup> and summing over the bcc lattice,<sup>48</sup>

$$\langle \Delta\nu^2 \rangle_{av} = 22.1 \hbar^{-2} G^2 (\langle S_x^2 \rangle_T - \langle S_x \rangle_T^2), \quad (15)$$

with  $G = g^2 \mu_B^2 / d^3$ , where  $d$  is the  $\text{Eu}^{2+}$ - $\text{Eu}^{2+}$  nearest-neighbor separation and the subscript  $T$  refers to the thermal average. With small  $H_A/T$  in  $\text{Eu}(\text{NH}_3)_6$ , this yields a full width at half-maximum (or linewidth) of the approximately Gaussian distribution

$$\Delta\nu_{1/2} = 2.35 (\langle \Delta\nu^2 \rangle_{av})^{1/2} \approx 2300 \text{ MHz}$$

corresponding to an energy width of 110 mK.

The relaxation-rate constant is taken as

$$\omega_R = \frac{2\pi}{\hbar} \sum_j [J + \frac{1}{4} G_{jk} (1 - 3\alpha_{jk}^2)]^2 P(E), \quad (16)$$

and should be independent of temperature except for the  $P(E)$  temperature dependence as shown in Eq. (15). Squaring and averaging over the polycrystal, using the dipolar sum, and assuming  $z$  nearest neighbors for the exchange term,

$$\omega_R = (2\pi/\hbar) (zJ^2 + 0.61 G^2) P(E). \quad (17)$$

For the probability  $P(M_k \rightarrow M'_k)$  in Eq. (13), the sum over  $M_b$  is valid only if the ionic levels are equally separated by the external field. If the crystal field is large enough so that the transition energies differ by more than about an ionic linewidth,

then the energy-conserving Hamiltonian demands that only one term be in the sum. In the Van Vleck case of equal splitting (denoted by ML for multi-level), if  $M_k \rightarrow M_k - 1$ , then for the  $j$  ions  $M_b \rightarrow M_b + 1$ ,  $M_b + 1 \rightarrow M_b + 2$ , etc., are allowed. For non-equal splittings (denoted by SL for single level), if  $M_k \rightarrow M_k - 1$ , then only  $M_k - 1 \rightarrow M_k$  is possible for the  $j$  ions.  $P(E)$  also changes depending on the mechanism causing the differences in the ionic transition energies. If the cubic crystal-field splittings are comparable to the dipolar interactions, the linewidth exhibits broadening.<sup>49</sup> A calculation using the  $B_4$  parameter for  $\text{CaF}_2:\text{Eu}^{2+}$  indicates an increase of about 100% in the  $\text{Eu}(\text{NH}_3)_6$  linewidth. Typical  $\text{Eu}^{2+}$  axial splitting terms are less important. The ML model should be the proper one to use here, although the results obtained assuming SL will also be given.

The calculated ML spectrum at an applied field  $H_A = 5.7$  kOe and temperature  $T = 1.20$  K [denoted by (5.7, 1.20)] yields a net ionic field  $H_N$  of about 4.9 kOe with a relaxation rate  $\omega_R \approx 70 \times 10^6 \text{ sec}^{-1}$  (see Fig. 10). Extrapolating to zero  $H_N/T$ , one obtains  $\omega_R(0) \approx 50 \times 10^6 \text{ sec}^{-1}$ . Errors for  $H_N$  and  $\omega_R$  for this data are estimated to be  $\pm 0.3$  kOe and  $\pm 20 \times 10^6 \text{ sec}^{-1}$ , respectively. The correlation between the two variables is slight.

The net field  $H_N$  observed at an ion is given by

$$H_N = H_A - \left(\frac{8}{3}\pi - N\right)M, \quad (18)$$

with the first term in parentheses corresponding to the demagnetization plus Lorentz fields for the disk-shaped absorber, and the second term accounting for any exchange field  $H_E = NM$ . The magnetization  $M$  is a function of  $H_N$  and  $T$  through a Boltzmann distribution. With  $M$  equal to 150 Oe in the  $S_z = -\frac{7}{2}$  state, the observed  $H_N$  for the (5.7, 1.20) data corresponds to  $N \approx 0$ . With  $SR \equiv -\langle S_z \rangle / 3.5 = 0.64$ , an upper limit on the paramagnetic value of exchange field at  $T = 0$  is given by  $|H_E(0)| \leq 0.5$  kOe. For ferromagnetic exchange, this corresponds to an upper limit on the Curie temperature  $T_C$  of about 0.1 K. For antiferromagnetic exchange, the paramagnetic Curie temperature  $|\Theta_N| \leq 0.1$  K. This value of  $\Theta_N$  is much more positive than that obtained from the susceptibility measurements - 5 K. From simple molecular-field theory,<sup>50</sup>  $T_N \leq |\Theta_N|$  for antiferromagnetic exchange with the bcc magnetic lattice. Thus, the ordering temperature in  $\text{Eu}(\text{NH}_3)_6$  should be less than 0.1 K, in contrast to the magnetization measurements indicating a ferromagnetic ordering temperature of 5.5 K. This would apparently be the lowest-ordering temperature in any  $\text{Eu}^{2+}$  compound.<sup>37</sup>

The data at 4.2 K and various  $H_A$  (see Fig. 9) indicate  $\omega_R$  is as expected roughly constant, including the slight effect of the  $H_N/T$  dependence of  $P(E)$ . The fairly good fit at (4.2, 4.2) using

the same  $\omega_R(0)$  as at larger fields is in contrast to the results obtained in  $\text{CaF}_2:\text{Eu}^{2+}$  at this field, where a much larger  $\omega_R$  had to be employed due to assumed cross-relaxation processes.<sup>42</sup> For the (0, 4.2) data, the plotted curve in Fig. 9 assumes SL and isotropic nuclear radiation, but that the  $M_S$  states are pure. The derived rate is then about  $300 \times 10^6 \text{ sec}^{-1}$ . Using ML,  $\omega_R \approx 50 \times 10^6 \text{ sec}^{-1}$ , or about the same as for the  $H_A \neq 0$  data. Fitting single Lorentzians to the  $H_A = 4.2$  kOe and  $H_A = 0$  data, the same FWHM is obtained in each case. The excellence of the fits indicates that these spectra (and all zero-field spectra) are Lorentzian in shape. The added spin-Hamiltonian terms and the overlapping ionic levels in zero field make a proper analysis difficult.

The ( $H_A$ , 1.2) intermediate-field data (Fig. 10) exhibit fitting parameter linewidths some 10% larger than the high-temperature data. Since no broadening is observed at (60, 1.2), quadrupole splitting can be ruled out. The increased linewidth is most likely due to locally varying  $H_{\text{eff}}$ , either due to a variation in  $\langle S_z \rangle$  due to crystal fields, or to the shape-dependent demagnetizing field in the various polycrystals. If the latter is true, then the average  $H_N$  is slightly larger than for an external field perpendicular to a uniform infinite disk.

Numerous spectra were obtained for sample I in applied fields. These data had very good statistics, and although saturation effects were prominent, an ISS dependent on  $T$  could be observed. The shift, as determined from the steep outer slopes, is about -0.12 mm/sec from 1.2 to 4.2 K. This is in reasonable agreement with the zero-field single-Lorentzian data in Fig. 5, considering that the relaxation data were first folded and then analyzed. The apparent independence of  $H_N$  rules out quadrupole splitting, crystal-field perturbation of the ionic levels, or  $\vec{I} \cdot \vec{S}$  terms in the Hamiltonian as possible causes of the ISS. There is a small asymmetry in the depths of the two central peaks for various  $SR \approx 0.58$  data, with the more positive velocity peak slightly broader and shallower. All samples showed this anomaly, so impurity effects can be ignored. The asymmetry anomaly could be caused by slightly differing hyperfine fields and isomer shifts characteristic of  $\text{Eu}(\text{NH}_3)_6$ .

Using the SL relaxation model, the (16.7, 4.2) data for sample J (Fig. 9) can be fit well with  $\omega_R \approx 250 \times 10^6 \text{ sec}^{-1}$ , and  $H_N \approx 14.1$  kOe, instead of the parameters shown in Fig. 9. This would imply an antiferromagnetic exchange field at  $SR = 1$  of  $H_E(0) \approx -3.4$  kOe. At lower  $H_A$  and 4.2 K, however, the calculated spectra are somewhat too broad, implying that the relaxation rate should increase. In addition, for the ( $H_A$ , 1.2) data, a

much different exchange field must be used if  $\omega_R(0)$  is taken as the 4.2-K value:  $H_E(0) \approx -1.0$  kOe.

This apparent variation in exchange field is probably an artifice of the model, since for all sample  $J$  data  $H_N/H_A \approx 0.8$ . It appears that even allowing  $\omega_R$  to vary at low temperature, no satisfactory fit can be obtained with the high temperature  $H_E(0)$ . The SL model seems unsatisfactory.

With the exchange Hamiltonian for an ion  $i$ ,

$$\mathcal{H}_{ex} = -2 \sum_j J_{ij} \vec{S}_i \cdot \vec{S}_j, \quad (19)$$

assuming that only  $z=8$  nearest neighbors are involved in the exchange process, then

$$J \equiv J_{ij} = \mu_B H_E(0) / zS.$$

Thus,

$$|J| < 1.0 \times 10^{-7} \text{ eV} = 1.2 \text{ mK}.$$

Inserting the various parameters into Eq. (17), the theoretical relaxation rates are

$$\begin{aligned} \omega'_R(0) &= 88 \times 10^6 \text{ sec}^{-1} \text{ (dipolar terms only),} \\ \omega'_R(0) &= 170 \times 10^6 \text{ sec}^{-1} \text{ (dipolar plus limiting} \\ &\quad \text{value of exchange, } z=8). \end{aligned}$$

The dipolar-only rate agrees well with the experimental value  $\omega_R(0) \approx (50 \pm 15) \times 10^6 \text{ sec}^{-1}$ , since (a) crystal-field terms will decrease  $\omega'_R$  and (b) correction for (slight) saturation will increase  $\omega_R(0)$ . In  $\text{Fe}(\text{NH}_4)(\text{SO}_4)_2 \cdot 12\text{H}_2\text{O}$ , the theoretical relaxation rate was about twice the experimental, with the exchange term dominating.<sup>46</sup>

It is worthwhile to consider the possibilities of other corrections to the relaxation rate. A small exchange field has a marked effect on the relaxation rate through the  $J^2$  dependence of  $\omega_R$ . Exchange also affects  $\omega_R$  through  $P(E)$ , because of the phenomenon of exchange narrowing. Using the upper limit on  $H_E(0)$ , the Anderson-Weiss formulas,<sup>51</sup> and Anderson's curves,<sup>52</sup> the ionic linewidth is calculated to be within a few percent of the dipolar-only width. The hyperfine splitting of the electronic states is of the order of a few mK and can be neglected.

#### F. Exchange Considerations

The lack of significant magnetic exchange interactions in  $\text{Eu}(\text{NH}_3)_6$  is unexpected since the high electrical conductivity would be expected to promote exchange. Consider first the localized indirect mechanism.<sup>53</sup> The nearest-neighbor interaction ( $J_1$ ) depends on the virtual excitation of a  $4f$  electron to the  $5d$  band, with the  $d$ - $f$  overlap at the nearest-neighbor site providing the exchange terms. For the Eu chalcogenides, the overlap dependence of the exchange constant on distance is given by

$$J_1(R) = J_1(R_0) e^{-8R/R_0}, \quad (20)$$

with  $J_1(R_0)$  the constant for  $\text{EuO}$ , with a nearest-neighbor distance of  $R_0$ . In  $\text{Eu}(\text{NH}_3)_6$  the overlap should be less, both because of the increased  $R$  and the directional aspect of the  $5d$ - $t_{2g}$  wave functions in  $\text{Eu}(\text{NH}_3)_6$ , which are not directed towards the nearest-neighbor cations as in the chalcogenides. Ignoring the latter aspect, the differences in excitation energy, and number of nearest neighbors, and comparing the hexammine ( $h$ ) to the oxide,

$$J_1(R_h) \approx 10^{-4} J_1(R_0),$$

with  $R_h = 8.27 \text{ \AA}$ ,  $R_0 = 3.64 \text{ \AA}$ .

Since the oxide orders at about 70 K, the hexammine critical temperature is predicted to be less than 0.1 K, in good agreement with the experimental results. The next-nearest-neighbor interaction ( $J_2$ ) proceeds via a cation-anion-anion-cation interaction, and should be very small.<sup>54</sup>

The long-range RKKY interaction from Eq. (7) leads to a paramagnetic Curie temperature  $\Theta_P$  given by<sup>55</sup>

$$\Theta_P = \frac{-3\pi Z^2 J_{sf}^2 S(S+1)}{4k_F E_F} \sum_{n \neq m} F(2k_F R_{nm}) \quad (21)$$

with

$$F(x) = (x \cos x - \sin x) / x^4,$$

where  $Z$  is the number of conduction electrons per atom,  $k_F$  and  $E_F$  are the Fermi wave vector and energy, and  $R_{nm}$  is the interatomic distance between  $\text{Eu}^{2+}$  ions. For the generally used spherical Fermi surface, the summation is independent of lattice constant since  $k_F a_0$  is independent of  $a_0$ . Barring a null in the sum, the experimental value of  $\Theta_P$  requires  $Z$  or  $J_{sf}$  to be small. Assuming at high temperatures a negligible  $s$  occupation of the conduction band, from the ISS data the measured shift at low temperatures corresponds to less than 0.02  $s$  electrons per  $\text{Eu}^{2+}$  ion. This should still lead to a substantial ferromagnetic interaction.<sup>56</sup> Another model<sup>1</sup> envisions the conduction electrons to be generally outside the ammonia cage surrounding the  $\text{Eu}^{2+}$  ion. Due to the short-range nature of  $J_{sf}$ , this would substantially reduce  $\Theta_P$ . A third possibility is that the RKKY and short-range mechanisms approximately cancel at 1.2 K. From the constancy of  $\omega_R$  from 4.2 to 1.2 K (ML model), this is unlikely.

#### G. Conclusion

The experimentally derived Eu hyperfine parameters in  $\text{Eu}(\text{NH}_3)_6$  correlate well with the normal  $4f^7$  configuration expected for  $\text{Eu}^{2+}$ . Our results strongly indicate that  $\text{Eu}(\text{NH}_3)_6$  is not magnetically ordered at temperatures down to 1.2 K, and an ordering temperature of about 0.1 K is predicted. Previously reported inferences of magnetic ordering may have been due to sample impurities.

The temperature dependence of the Mössbauer recoil-free fraction is found to be in very good agreement with a simple Debye model, yielding a Debye temperature of 43 K for  $\text{Eu}(\text{NH}_3)_6$ . The unusual and interesting variations in linewidth and isomer shift have been explained with reasonable models, but the full interpretation must await other corroborative experimental work.

Experimental data obtained in applied magnetic fields were used to derive the saturation hyperfine field for  $\text{Eu}(\text{NH}_3)_6$ . The result - 322 kOe corresponding to a fully magnetized  $\langle S_x \rangle = -\frac{7}{2}$  state, is very similar to values reported for other  $\text{Eu}^{2+}$  compounds and can be interpreted as arising from  $4f^7$  core polarization. The complicated Mössbauer spectra observed in moderate applied fields can be reproduced very well using spin-relaxation theory. The extracted spin-spin relaxation rate is in good agreement with calculations based upon dipolar interactions and no exchange field at the Eu ion.

It would be very useful to have more x-ray diffraction data below 77 K for detailed crystal-structure information, and ESR measurements to detect possible site symmetry changes and exchange interactions. Current Mössbauer studies being carried out in our laboratory will investigate the effects of Eu dilution in nonmagnetic isomorphous hexammine lattices.

Since the completion of this work, another study<sup>57</sup> of the Mössbauer effect in  $\text{Eu}(\text{NH}_3)_6$  has appeared. The spectra taken at various temperatures without an external magnetic field indicate little temperature dependence of the strength of the resonance. There are three chemical phases present in the sample studied, two divalent and one trivalent. The divalent phase with the highest Debye temperature, which the authors consider to be the hexammine, exhibits the same isomer shift at 77 K as found in the earlier impure samples discussed in this paper. This phase orders magnetically between 4.2 and 20.4 K. The second divalent phase exhibits the properties ascribed here to  $\text{Eu}(\text{NH}_3)_6$ . The authors consider this phase to represent Eu dissolved in ammonia, however no such phase has been identified by others.

#### ACKNOWLEDGMENTS

Appreciation is gratefully extended for the many hours of computer time made available by the NIH Biomedical Research Facility at Carnegie-Mellon University. Thanks are also due to Dr. T. X. Carroll for assistance and advice in several aspects of the work and to Dr. R. L. Cohen for making available a preprint of his work prior to publication.

\*This work has been supported by the U.S. Atomic Energy Commission.

<sup>1</sup>H. Oesterreicher, N. Mammano, and M. J. Sienko, *J. Solid State Chem.* **1**, 10 (1969).

<sup>2</sup>J. C. Nickerson, R. M. White, K. N. Lee, R. Backmann, T. H. Geballe, and G. W. Hull, Jr., *Phys. Rev. B* **3**, 2030 (1971).

<sup>3</sup>G. Williams and L. L. Hirst, *Phys. Rev.* **185**, 407 (1969).

<sup>4</sup>L. L. Hirst and E. R. Seidel, *J. Phys. Chem. Solids* **31**, 857 (1970).

<sup>5</sup>S. Dickman, N. J. Senozan and R. L. Hunt, *J. Chem. Phys.* **52**, 2657 (1970).

<sup>6</sup>P. R. Marshall and H. Hunt, *J. Phys. Chem.* **60**, 732 (1956).

<sup>7</sup>M. J. Sienko, in *Metal-Ammonia Solutions*, edited by G. Lepoutre and M. J. Sienko (Benjamin, New York, 1963), p. 26.

<sup>8</sup>E. C. Franklin, *The Nitrogen System of Compounds* (Reinhold, New York, 1935), p. 21.

<sup>9</sup>J. A. Morgan and J. C. Thompson, *J. Chem. Phys.* **47**, 4607 (1967).

<sup>10</sup>W. J. McDonald, J. C. Thompson, and D. E. Bowen, *Bull. Am. Phys. Soc.* **9**, 735 (1964).

<sup>11</sup>A. H. Muir, *Tables and Graphs for Computing Debye-Waller Factors in Mössbauer Effect Studies* (Atomics International, Canoga Park, Calif., 1962).

<sup>12</sup>J. Heberle and S. Franco, *Z. Naturforsch. A* **23**, 1439 (1968).

<sup>13</sup>S. Franco and J. Heberle, *Z. Naturforsch. A* **25**, 134 (1970).

<sup>14</sup>K. A. Hardy, F. T. Parker, and J. C. Walker, *Nucl. Instrum. Methods* **86**, 171 (1970).

<sup>15</sup>F. T. Parker, K. A. Hardy, and J. C. Walker, *Phys. Rev. C* **3**, 841 (1971).

<sup>16</sup>S. Hufner and J. H. Wernick, *Phys. Rev.* **173**, 448 (1968).

<sup>17</sup>G. K. Wertheim, *Phys. Rev.* **121**, 63 (1961).

<sup>18</sup>J. Korrington, *Physica (Utr.)* **16**, 601 (1950).

<sup>19</sup>C. P. Slichter, *Principles of Magnetic Resonance* (Harper and Row, New York, 1963), p. 124.

<sup>20</sup>J. B. Horak and A. W. Nolle, *Phys. Rev.* **153**, 372 (1967).

<sup>21</sup>K. R. Lea, M. J. M. Leask, and W. P. Wolf, *J. Phys. Chem. Solids* **23**, 1381 (1962).

<sup>22</sup>M. M. Abraham, L. A. Boatner, Y. Chen, J. L. Kolopus, and R. W. Reynolds, *Phys. Rev. B* **4**, 2853 (1971).

<sup>23</sup>W. Low, *Paramagnetic Resonance in Solids* (Academic, New York, 1960), p. 119.

<sup>24</sup>S. U. Cheema and M. J. A. Smith, *J. Phys. C* **4**, 1231 (1971).

<sup>25</sup>L. Asch, J. P. Adloff, J. M. Friedt, and J. Danon, *Chem. Phys. Lett.* **5**, 105 (1970).

<sup>26</sup>A. R. Bates and K. W. H. Stevens, *J. Phys. C* **2**, 1573 (1969).

<sup>27</sup>N. Mammano and M. J. Sienko, *J. Am. Chem. Soc.* **90**, 6322 (1968).

<sup>28</sup>S. Hufner, J. Brinkman, and G. Creelius, *Phys. Lett. A* **36**, 367 (1971).

<sup>29</sup>W. J. McDonald and J. C. Thompson, *Phys. Rev.* **150**, 602 (1966).

<sup>30</sup>W. W. Lemaster and J. C. Thompson, *J. Solid State Chem.* **4**, 163 (1972).

<sup>31</sup>S. Ofer, I. Nowik, and S. G. Cohen, in *Chemical Applications of Mössbauer Spectroscopy*, edited by V. I. Goldanskii and R. H. Herber (Academic, New York, 1968), p. 493.

<sup>32</sup>G. Petrich, S. von Molnár, and T. Penney, *Phys. Rev. Lett.* **26**, 885 (1971); T. Penney, M. W. Shafer, and J. B.

Torrance, *Phys. Rev. B* **5**, 3669 (1972); J. B. Torrance, M. W. Shafer, and T. R. McGuire, *Phys. Rev. Lett.* **29**, 1168 (1972).

- <sup>33</sup>G. Groll, Z. Phys. **243**, 60 (1971).
- <sup>34</sup>O. Berkooz, J. Phys. Chem. Solids **30**, 1763 (1969).
- <sup>35</sup>T. J. Menne, D. P. Ames, and S. Lee, Phys. Rev. **169**, 333 (1968); T. J. Menne, Phys. Rev. **180**, 350 (1969).
- <sup>36</sup>H. H. Wickman, J. H. Wernick, R. C. Sherwood, and C. F. Wagner, J. Phys. Chem. Solids **29**, 181 (1968).
- <sup>37</sup>G. J. Enholm, T. E. Katila, O. V. Lounasmaa, P. Reivari, G. M. Kalvius, and G. K. Shenoy, Z. Phys. **235**, 289 (1970).
- <sup>38</sup>J. M. Baker and F. I. B. Williams, Proc. R. Soc. A **267**, 283 (1962).
- <sup>39</sup>S. Ofer, I. Nowik, and S. G. Cohen, Ref. 32, p. 439.
- <sup>40</sup>C. E. Johnson, in *Hyperfine Interactions in Excited Nuclei*, edited by G. Goldring and R. Kalish (Gordon and Breach, New York, 1971), p. 805.
- <sup>41</sup>S. Ofer, I. Nowik, and S. G. Cohen, Ref. 32, p. 445.
- <sup>42</sup>H. H. Wickman, Phys. Lett. A **31**, 29 (1970).
- <sup>43</sup>H. H. Wickman, M. P. Klein, and D. A. Shirley, Phys. Rev. **152**, 345 (1966).
- <sup>44</sup>J. H. Van Vleck, Phys. Rev. **74**, 1168 (1948).
- <sup>45</sup>H. H. Wickman, in Ref. 31, p. 602.
- <sup>46</sup>A. J. F. Boyle and J. R. Gabriel, Phys. Lett. **19**, 451 (1965).
- <sup>47</sup>K. Kambe and T. Usui, Prog. Theor. Phys. **8**, 302 (1952).
- <sup>48</sup>J. E. Jones and A. E. Ingham, Proc. Roy. Soc. Lond. **107**, 636 (1925).
- <sup>49</sup>R. Bersohn, J. Chem. Phys. **20**, 1505 (1952).
- <sup>50</sup>A. H. Morrish, *The Physical Principles of Magnetism* (Wiley, New York, 1965), p. 447.
- <sup>51</sup>P. W. Anderson and P. R. Weiss, Rev. Mod. Phys. **25**, 269 (1953).
- <sup>52</sup>P. W. Anderson, J. Phys. Soc. Jap. **9**, 316 (1954).
- <sup>53</sup>T. Kasuya, IBM J. Res. Dev. **14**, 214 (1970).
- <sup>54</sup>J. B. Goodenough, *Magnetism and the Chemical Bond* (Wiley, New York, 1963), p. 184.
- <sup>55</sup>P. de Gennes, C.R. Acad. Sci. (Paris) **247**, 1836 (1958).
- <sup>56</sup>D. C. Mattis, *The Theory of Magnetism* (Harper and Row, New York, 1965), p. 204.
- <sup>57</sup>J. P. Brown, R. L. Cohen, and K. W. West, Chem. Phys. Lett. **20**, 271 (1973).